A New Simple and Effective Procedure for SiPM Electrical Parameter Extraction

Davide Marano, Giovanni Bonanno, Salvatore Garozzo, Alessandro Grillo, and Giuseppe Romeo

***Abstract*— Silicon photomultipliers (SiPMs) are emerging semiconductor-based photosensors, addressing the challenge of low-light detection down to the single-photon counting level. A design of high-performance front-end electronics for SiPM readout requires the development of accurate electrical models. Numerous SiPM reliable models have matured in recent years; however, circuit parameter extraction is rather cumbersome and involves extensive measurement steps to be performed. Starting from a recently developed model of the SiPM device coupled to the conditioning electronics, a new effective analytical procedure is, here, devised for extracting the SiPM model parameters from experimental measurements. The proposed extraction technique is applied to a 3 × 3-mm^2 SiPM sensor, and is validated by comparing SPICE simulations and measurement results. Independent cross-check validation based on experimental tests corroborates the effectiveness of the adopted extraction procedure.**

***Index Terms*— Analytical model, circuit parameters, front-end electronics, pulse waveform, transient response.**

I. Introduction

IN LIGHT of the contemporary evolution of astrophysics, nuclear science and medical imaging, the development of new silicon photomultiplier (SiPM) detectors is being devoted an ever-increasing amount of attention in recent years. The number of scientific and technical applications which benefit from the peculiar advantages of solid-state sensors is continuously growing over time, fostered by the rapid industrial advancement of modern semiconductor technologies.

SiPMs basically consist of a parallel array of single-photon avalanche photodiodes operating above breakdown (in the so-called Geiger-mode) in series with an integrated quenching or ballast resistance. In principle, for a SiPM proper operation, a biasing circuit and a read-out amplifier are required, as schematically shown in the simplified diagram in Fig. 1.

In the steady-state condition, no current flows through the device terminals, and the external supply V_{BIAS} sets the SiPM operating point at a voltage which is typically 10-20% greater than its breakdown potential. When an optical photon strikes the active surface of the n-th photodiode, the device microcell undergoes a Geiger discharge and produces a short pulse current, $i_n(t)$, resulting in a voltage pulse signal at the SiPM output node, $v_n(t) = GR_L i_n(t)$, where G is the avalanche multiplication factor and R_L is the sensing resistance. If a given number of photons triggers N_f avalanches in N_f different pixels, then the overall sensor response would be the analog superposition of N_f individual pulse shapes. Under the assumption of uniform gain among the individual microcells, N_f triggered pixels would deliver an output voltage signal expressed as

$$v(t) = \sum_{n=1}^{N_f} v_n(t) = \sum_{n=1}^{N_f} GR_L i_n(t) = N_f\,[GR_L i(t)], \quad (1)$$

hence theoretically permitting the detection and measurement of optical signals at the single photon counting level.

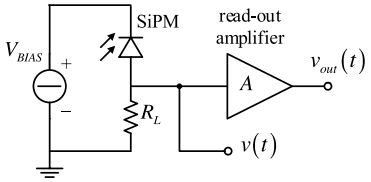

Fig. 1. Schematic overview of a typical SiPM read-out circuit.

In order to exploit the excellent intrinsic SiPM timing resolution, the development of specialized, highly integrated read-out electronics is required. However, the number of front-end architectures specifically designed for SiPM read-out is fairly poor, and considerable effort is thus being involved in finding newer and more performing solutions in terms of dynamic speed and time resolution. To this purpose, a substantial benefit for circuit designers is represented by the possibility of performing accurate circuit-level simulations of the SiPM detector coupled to the conditioning electronics, allowing to choose the optimal characteristics of the front-end systems for optimizing overall time performance.

In this scenario, the rising number of emerging applications demanding best theoretical dynamic speed and single-photon time resolution, as well as the contextual request for suitable integrated front-end electronics, have recently provided motivation and stimuli for in-depth research studies on the SiPM output dynamic response [1]–[12], allowing a detailed analytical description of the device behavior.

A traditionally accepted electrical model of a SiPM detector is shown in Fig. 2. The model is able to simulate the discharge of N_f active pixels over a number N of total microcells.

Manuscript received January 27, 2016; accepted February 14, 2016. Date of publication February 18, 2016; date of current version April 8, 2016. This work was supported in part by the ASTRI flagship project, financed by the Italian Ministry of Education, University and Research (MIUR) and led by the Italian National Institute for Astrophysics (INAF). The associate editor coordinating the review of this paper and approving it for publication was Dr. Richard T. Kouzes.

The authors are with INAF, Osservatorio Astrofisico di Catania, Catania 95123, Italy (e-mail: davide.marano@oact.inaf.it; giovanni.bonanno@oact.inaf.it; salvatore.garozzo@oact.inaf.it; alessandro.grillo@oact.inaf.it; giuseppe.romeo@oact.inaf.it).

Digital Object Identifier 10.1109/JSEN.2016.2530848

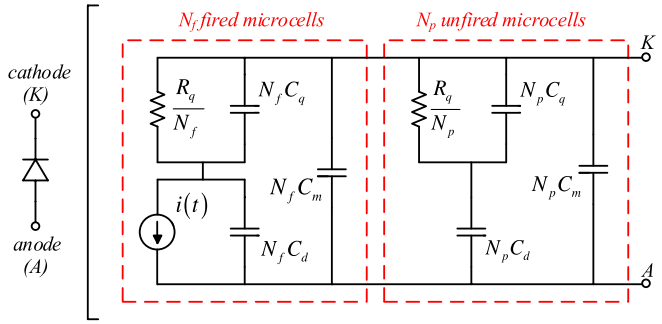

Fig. 2. Traditional electrical model of a SiPM detector.

The circuit is divided into an active part for the N_f fired pixels and a passive block for the remaining $N_p = N\text{-}N_f$ unfired microcells. For an individual pixel, C_d is the junction capacitance of the diode depletion layer, R_q and C_q are respectively the ballast resistance and stray capacitance, while C_m accounts for all interconnect capacitances across the SiPM terminals.

The Geiger discharge of the single firing microcell, caused by either an impinging photon or thermal carriers generation, is mimicked by the time-dependent source $i(t)$, simulating the photodiode exponential decay current and expressed as

$$i(t) = \frac{Q}{\tau_d} e^{-\frac{t}{\tau_d}}, \tag{2}$$

where τ_d is the quenching time constant of the avalanche discharge and Q is the overall amount of charge delivered by the fired pixel, which is represented by the integral of the photodiode current over time and calculated as the product between the excess bias voltage V_{OV} and the pixel capacitance C_{pixel}

$$\begin{aligned} Q &= \int_0^{+\infty} i(t)\, dt = C_{pixel} V_{OV} \\ &= \left(C_d + C_q\right)(V_{BIAS} - V_{BD}), \end{aligned} \tag{3}$$

being V_{BD} the device breakdown potential.

The number of unit electron charges originated in response to a photon absorption (or a thermally ignited avalanche), denotes the multiplication factor G of the Geiger discharge and is usually referred to as the SiPM gain, whose typical expression as a function of the operating voltage is then

$$G = \frac{Q}{q} = \frac{C_d + C_q}{q}(V_{BIAS} - V_{BD}). \tag{4}$$

where q denotes the elementary electron charge.

The effectiveness of the SiPM model, along with its ability to perform reliable software simulations, is strongly related to the choice of the circuit parameters, whose derivation strategy hence assumes a significant role in establishing predictive capability of the adopted model. Despite the inherent simplicity and accuracy of the SiPM model in Fig. 2, the related parameter extraction methodology is somewhat complex and burdensome, and needs extensive and time-consuming measurement steps to be performed [13]–[17]. More specifically:

a) the breakdown voltage V_{BD} is estimated by the measured detector current as a function of the reverse bias voltage, or else from the extrapolation of the x-axis intercept of a linear fit in a gain plot against the operating voltage;
b) parameter τ_d is evaluated from the measured rise time of the amplified SiPM signal;
c) resistor R_q is obtained through the slope of the static I-V characteristics of the device in its forward region;
d) the terminal capacitance C_{pixel} is extracted by evaluating the overall charge injected by the fired pixels in a signal charge histogram, or alternatively through the slope of a linear fit in a gain plot versus the operating voltage;
e) the individual capacitive components C_d and C_q, and the grid parasitic capacitance C_p, are assessed by fitting the complex impedance of the SiPM model to the measured impedance of the reverse-biased device.

In addition, parameter extraction does not take into account the effect of the read-out electronics on the shape of the SiPM response, which might have a non-negligible influence on the value of the estimated model parameters.

In the following, a new effective and straightforward methodology for extracting the SiPM model parameters is devised, relying on two simpler measurement steps:

a) determination of R_q by means of a linear fit to the measured forward I-V characteristics;
b) extraction of all remaining electrical parameters through the measurement and analytical data fitting of the amplified SiPM transient response.

The proposed procedure is based on a recently adopted full model of the SiPM detector with its coupled read-out amplifier [1], and is then validated and cross-checked by comparison with experimental results.

The remainder of the paper is organized as follows. In Section II, the enhanced SiPM model resulting from coupling the device to its read-out amplifier is briefly reviewed. The novel procedure for SiPM parameter extraction is addressed in Section III. In Section IV, experimental validation of the adopted strategy is performed. Section V provides cross-check results corroborating the effectiveness of the proposed methodology. Finally, the authors' conclusions are drawn in Section VI.

II. Review of the Full SiPM Analytical Model

Fig. 3 depicts the linear small-signal circuit of the electrical model of the SiPM detector when coupled to its read-out electronics. The SiPM equivalent circuit is directly derived from the model in Fig. 2 endorsing capacitances $N_f C_m$ and $N_p C_m$ into the single capacitive contribution $C_p = NC_m$. The equivalent circuit of the front-end electronics is based on the typical single-pole model of a generic read-out amplifier, where R_{in} and C_{in} are respectively the equivalent input resistance and capacitance, $g_m R_{out}$ is the DC gain A, while the product $R_{out} C_{out}$ represents the reciprocal of the 3dB cut-off angular frequency resulting from dominant-pole approximation.

The trans-resistive small-signal transfer function of the circuit model in Fig. 3 in the complex s-frequency

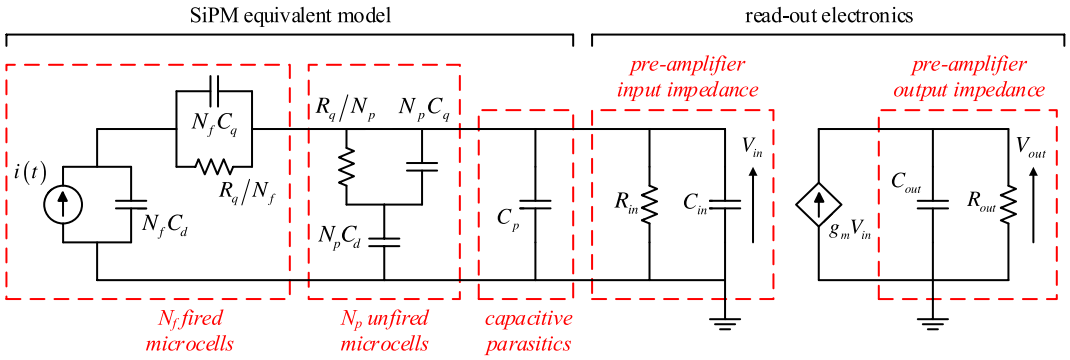

Fig. 3. Linear small-signal equivalent model of the SiPM detector coupled to the front-end electronics.

domain is

$$F(s) = \frac{V_{out}(s)}{I(s)} = F_0 \frac{1 + s\tau_z}{(1 + s\tau_{p1})(1 + s\tau_{p2})(1 + s\tau_{out})}, \tag{5}$$

with $F_0 = g_m R_{in} R_{out}$, and the circuit time constants given by

$$\tau_z = R_q C_q, \tag{6}$$

$$\tau_{p1} = R_q (C_d + C_q) + R_{in}(C_{in} + NC_d), \tag{7}$$

$$\tau_{p2} = \frac{R_{in} R_q [NC_d C_q + (C_{in} + C_p)(C_d + C_q)]}{R_q (C_d + C_q) + R_{in}(C_{in} + NC_d)}, \tag{8}$$

$$\tau_{out} = R_{out} C_{out}. \tag{9}$$

Solving (5) for $V_{out}(s)$, substituting the s-domain expression of $i(t)$ in (2), and then inverse Laplace transforming, the final SiPM single-photoelectron time response is derived as

$$v_{out}(t) = k\left(A_d e^{-\frac{t}{\tau_d}} + A_{p1} e^{-\frac{t}{\tau_{p1}}} + A_{p2} e^{-\frac{t}{\tau_{p2}}} + A_{out} e^{-\frac{t}{\tau_{out}}}\right), \tag{10}$$

in which the static multiplicative term is

$$k = F_0 Q = q F_0 G, \tag{11}$$

and the four exponential coefficients are expressed by

$$A_d = \frac{\tau_d(\tau_d - \tau_z)}{(\tau_d - \tau_{p1})(\tau_d - \tau_{p2})(\tau_d - \tau_{out})}, \tag{12}$$

$$A_{p1} = \frac{\tau_{p1}(\tau_{p1} - \tau_z)}{(\tau_{p1} - \tau_d)(\tau_{p1} - \tau_{p2})(\tau_{p1} - \tau_{out})}, \tag{13}$$

$$A_{p2} = \frac{\tau_{p2}(\tau_{p2} - \tau_z)}{(\tau_{p2} - \tau_d)(\tau_{p2} - \tau_{p1})(\tau_{p2} - \tau_{out})}, \tag{14}$$

$$A_{out} = \frac{\tau_{out}(\tau_{out} - \tau_z)}{(\tau_{out} - \tau_d)(\tau_{out} - \tau_{p1})(\tau_{out} - \tau_{p2})}. \tag{15}$$

The SiPM output response is a quadruple-exponential function exhibiting a rising (τ_d), quenching (τ_{p2}), and recovery (τ_{p1}) phase, and also accounting for the shaping effects of the coupled front-end electronics (τ_{out}).

The overall charge Q released by the triggered microcells and delivered to the output signal is proportional to the integral of the SiPM response over time, and is merely related to the pixel capacitance and applied excess bias voltage, as established in (3). This means that, for the same load resistance, R_{in}, and pre-amplifier gain factor, $g_m R_{out}$, the integral of $v_{out}(t)$ with respect to time should be independent of the frequency characteristics of the front-end electronics (τ_{out}). In fact,

$$\int_0^{+\infty} v_{out}(t)\,dt = k\left(A_d\tau_d + A_{p1}\tau_{p1} + A_{p2}\tau_{p2} + A_{out}\tau_{out}\right) = k \tag{16}$$

since the sum of the terms in round brackets equals unity.

The achieved expression for $v_{out}(t)$ in (10) also satisfies the initial- and final-value conditions, as

$$v_{out}(0) = k\left(A_d + A_{p1} + A_{p2} + A_{out}\right) = 0, \tag{17}$$

$$\lim_{t \to +\infty} v_{out}(t) = 0. \tag{18}$$

A remarkable advantage of the obtained analytical relationship of the SiPM output waveform is that it properly accounts for the effect of the coupled front-end electronics, modulating the shape of the basic SiPM pulse ($v(t)$ in Fig. 1) and playing a major role in determining time performance, dynamic range and photon counting resolution of the detection system independently of the particular fabrication technology. Indeed, relying on the general pre-amplifier macro-model in Fig. 3, the SiPM front-end electronics can be functionally associated to the major relevant model parameters regardless of the specific inner circuit topology and architecture.

Based on the above model and analytical analysis, the new procedure for SiPM parameter extraction is now developed.

III. Model Parameter Extraction Procedure

The first step of the proposed procedure consists in the determination of the quenching resistance R_q. Biasing the SiPM detector in its forward region, the resulting I-V characteristics should obey to the following law

$$V = \frac{R_q}{N} I + \eta V_T \ln\left(\frac{I}{N I_S}\right), \tag{19}$$

in which V_T and η are respectively the thermal voltage and the emission coefficient of the photodiode junction, and I_S is the photodiode reverse saturation current.

The SiPM forward I-V curves present two distinct parts: an initial phase when the current is governed by the typical diode exponential behavior as a function of the applied voltage, and a subsequent phase in which the quenching resistor becomes the dominant contribution and limits the forward current to an almost linear growth. The equivalent resistance R_q/N can thus be evaluated from the slope of the linear part, from which the quenching resistor value can be easily extracted.

As to the succeeding measurement step, referring to Fig. 1, the SiPM single-photoelectron response, $v_{out}(t)$, is recorded on a digital oscilloscope with the detector under test subjected to dark count events, ensuring the most probable event to be the firing of a single pixel. For a fixed external voltage V_{BIAS}, histograms of the maximum pulse heights are digitally captured according to the number of cells triggering for each event. Afterwards, events with equal number of fired cells are grouped and averaged to form a single pulse waveform.

Model parameters of the read-out section are obtained from the knowledge of the specific amplifier adopted. In particular, the input capacitance C_{in} is typically available from the manufacturer datasheet, whilst the input and output resistances, R_{in} and R_{out} respectively, along with the –3dB small-signal bandwidth f can be achieved from the simulation model once the desired amplifier configuration and closed-loop gain A are selected. Subsequently, transconductance g_m is derived from the equation $A = g_m R_{out}$, and capacitance C_{out} is evaluated by means of the well-known relationship

$$f = \frac{1}{2\pi R_{out} C_{out}}, \tag{20}$$

hence allowing the values of F_0 and τ_{out} to be determined.

At this point, a nonlinear regression technique is applied to the measured SiPM output response, and the collected data of $v_{out}(t)$ are fitted with a fourth-exponential function g obtained substituting expressions (11)-(15) into (10), yielding

$$v_{out} = g\left(G, \tau_d, \tau_{p1}, \tau_{p2}, \tau_z\right), \tag{21}$$

in order to find the unknown parameters G and τ_d, τ_{p1}, τ_{p2}, τ_z.

Once the three time constants τ_{p1}, τ_{p2}, and τ_z are evaluated, by means of the relevant analytical expressions in (6)-(8), the values of the three capacitors C_d, C_q, and C_p can be easily extracted according to the following relationships

$$C_d = \frac{\tau_{p1} - \tau_{in} - \tau_z}{R_q}, \tag{22}$$

$$C_q = \frac{\tau_z}{R_q}, \tag{23}$$

$$C_p = \frac{N R_{in}\left(\tau_{p2} - \tau_z\right) + R_q\left(\tau_{p2} - \tau_{in}\right)}{R_{in} R_q}, \tag{24}$$

where τ_{in} represents the product between R_{in} and C_{in}.

Finally, from the known value of G and using the estimated values of C_d and C_q in (22)-(23), the SiPM breakdown potential is easily obtained from (4) as

$$V_{BD} = V_{BIAS} - \frac{qG}{C_d + C_q}. \tag{25}$$

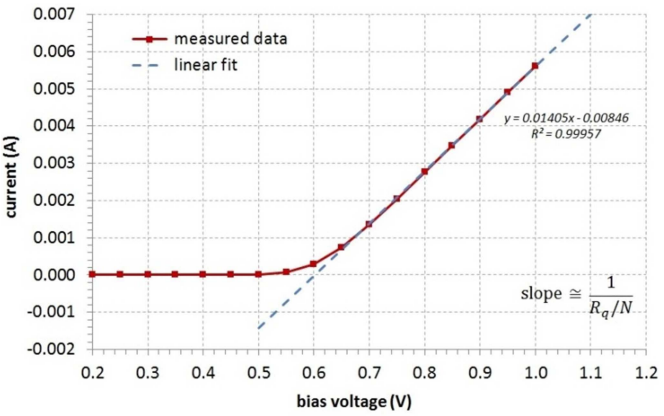

Fig. 4. Fitting of the linear part of the SiPM forward I-V characteristics, from which the value of the quenching resistor R_q is extracted.

IV. Validation of the Extraction Procedure

The adopted extraction procedure is exploited to derive the electrical model parameters of a 3×3-mm^2 multi-pixel photon counter detector supplied by Hamamatsu Photonics, featuring a 50-μm cell size and 3600 elementary pixels. The breakdown voltage declared in the manufacturer datasheet ranges around 65V at room temperature.

Data-fitting procedures are performed in the MATLAB environment using the command `lsqcurvefit()`, which enables measurement data arrays to be fitted with complex non-linear functions in least-squares sense.

The SiPM static I-V characteristics are illustrated in Fig. 4, along with a linear fitting regression applied to the measured data points corresponding to an operating voltage higher than 0.7V. By the slope of the linear fit, a value of 256.2kΩ is extracted for the quenching resistor R_q.

To obtain the remaining parameters of the SiPM model, the experimental apparatus illustrated in Fig. 1 is assembled, with $R_L = 50\Omega$ and $V_{BIAS} = 68$V. A THS3201 read-out pre-amplifier is used in non-inverting feedback configuration, with a 1-pF input capacitance and a ~40-dB nominal gain factor, for which a closed-loop bandwidth of ~50-MHz is achieved from simulations. The measured SiPM pulse waveforms are acquired on a Lecroy digital oscilloscope characterized by a 4-GHz bandwidth, a 40-GS/s sampling rate, and an intrinsic 0.5-mV baseline noise. SiPM single-photoelectron responses are captured with the detector lodged in a dedicated light-tight box to prevent accidental light exposure. Measurements are executed at room temperature.

The estimated parameters resulting from the fit between the experimental pulse waveform and the quadruple-exponential function in (21) are reported in Table I. Finally, according to the analytical expressions derived in Section III, the values of the SiPM model capacitances are calculated, together with the detector breakdown voltage. The extracted electrical parameters of the SiPM model in Fig. 2 are summarized in Table II.

To validate the above procedure, the circuit in Fig. 1 is implemented in SPICE using the SiPM model in Fig. 2 with the cascaded read-out pre-amplifier, as shown in Fig. 5.

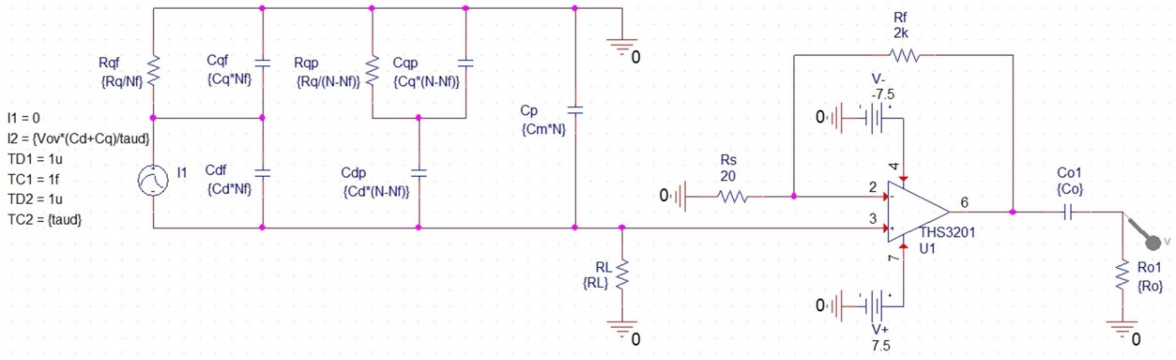

Fig. 5. Implemented SPICE-level model of the SiPM detector driven by a voltage non-inverting feedback amplifier.

TABLE I
PARAMETERS OF THE SiPM FITTING FUNCTION IN (21)

Parameter	Value
τ_d	(0.25±0.03) ns
τ_{p1}	(40.09±0.05) ns
τ_{p2}	(1.65±0.01) ns
τ_z	(3.04±0.02) ns
G	(1.68±0.03)×10^6

TABLE II
ELECTRICAL PARAMETERS OF THE SiPM MODELIN FIG. 2

Parameter	Value
R_q	(256.2±0.7) kΩ
C_d	(86.1±0.6) fF
C_q	(12.8±0.2) fF
C_p	(2.7±0.3) pF
V_{BD}	(65.2±0.1) V

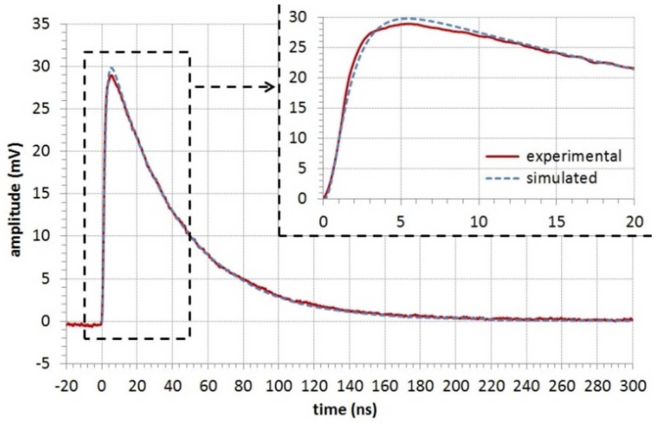

Fig. 6. Simulated and experimental SiPM single-photoelectron responses.

Comparison between the SPICE model simulations and the relevant experimental data is displayed in Fig. 6. As shown, a good fitting is achieved, confirming expectations and validating the proposed extraction procedure.

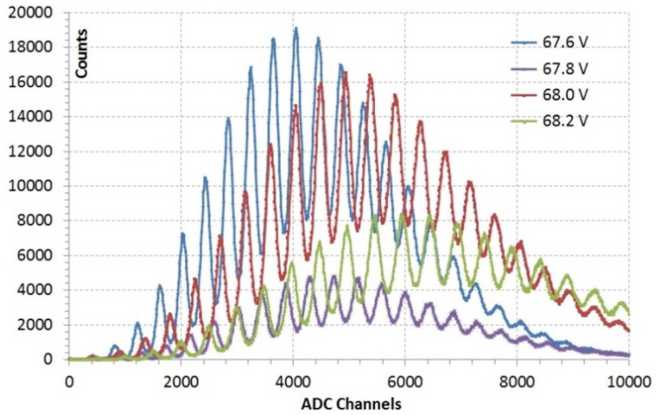

Fig. 7. Charge amplitude histograms at four different bias conditions.

V. EXPERIMENTAL CROSS-CHECK VALIDATION

In order to further corroborate the effectiveness of the proposed methodology, experimental measurements on the available SiPM device are also carried out following the traditional procedure, to derive some of the SiPM model parameters and compare the achieved results with those extracted in Section IV. In particular, charge measurements are accomplished for a given set of operating voltages, allowing to extract the SiPM gain G, pixel capacitance C_{pixel} and breakdown voltage V_{BD}.

To evaluate the detector gain at a given bias voltage, the integrated charge values generated by a multi-channel analyzer are filled into charge height histograms, and the average spacing between two adjacent curve peaks is computed in terms of ADC channels. As a consequence, accounting for the constant charge/channel rate, and scaling by the pre-amplifier gain factor, the SiPM gain is obtained for a fixed operating condition. During charge measurements, the SiPM device is illuminated with a PDL-200B pulsed diode laser triggering the device microcells. For each acquisition, laser radiation intensity and integration time windows are designed in order to attain a sufficiently large number of photoelectron peaks. Fig. 7 illustrates the SiPM charge measurements at four different bias voltages. The average spacing between succeeding peaks almost linearly increases with the operating conditions.

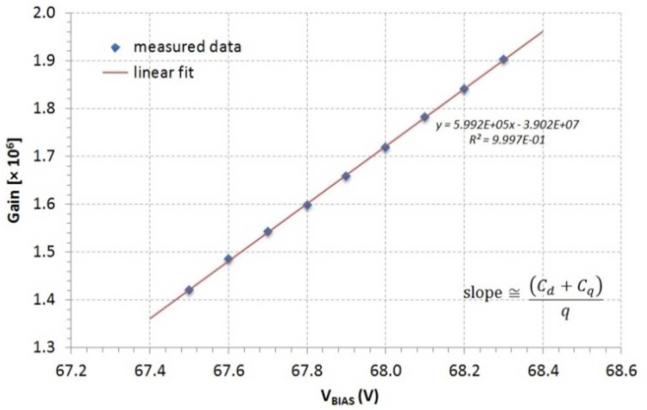

Fig. 8. Gain measurements as a function of the operating voltage. The linear fit allows to extrapolate the breakdown potential.

The SiPM measured gains for a few different bias voltages are plotted in Fig. 8. In particular, a value of $(1.72\pm0.05)\times10^6$ is estimated at $V_{BIAS} = 68$V, which is fairly compatible with the SiPM gain G extracted in Table I.

Through the slope of the linear fit in a gain graph as a function of the operating voltage, the SiPM pixel capacitance C_{pixel} can be appraised, in accordance with (4). From Fig. 8, a value of (98±1)fF is achieved, which is consistent with the extracted parameters C_d and C_q in Table II.

Lastly, the extrapolation of the x-axis intercept of the linear fit in Fig. 8 provides an estimate of the SiPM breakdown potential, as predicted in (4). As a result, a V_{BD} of (65.1±0.1)V is found, complying with the corresponding datum in Table II.

Therefore, the SiPM parameters extracted by the traditional measurement steps are verified to yield good agreement with those assessed following the simpler extraction methodology in Section IV, thus cross-checking the proposed procedure.

VI. Conclusion

In this contribution, an original and simple extraction procedure for deriving the electrical parameters of a SiPM detector has been presented, based on a recently available model of the SiPM device when coupled to its read-out electronics. After a brief review of the analytical analysis developed for determining the complete expression of the single-photoelectron output response, the novel extraction procedure has been proposed, entailing few simple and straightforward measurement steps. The adopted technique has been exploited to extract the electrical parameters of a 3mm×3mm Hamamatsu device and construct a SPICE-level model of the SiPM and related read-out circuit. Comparison between simulated and measurement data, along with experimental cross-check results, have confirmed the effectiveness of the new extraction procedure.

References

[1] D. Marano, G. Bonanno, S. Garozzo, A. Grillo, and G. Romeo, "New improved model and accurate analytical response of SiPMs coupled to read-out electronics," *IEEE Sensors J.*, vol. 16, no. 1, pp. 19–21, Jan. 2016.

[2] F. Villa, Y. Zou, A. Dalla Mora, A. Tosi, and F. Zappa, "SPICE electrical models and simulations of silicon photomultipliers," *IEEE Trans. Nucl. Sci.*, vol. 62, no. 5, pp. 1950–1960, Oct. 2015.

[3] S. Vinogradov, A. Arodzero, R. C. Lanza, and C. P. Welsch, "SiPM response to long and intense light pulses," *Nucl. Instrum. Methods Phys. Res. A, Accel. Spectrom. Detect. Assoc. Equip.*, vol. 787, pp. 148–152, Jul. 2015.

[4] D. Marano *et al.*, "Accurate analytical single-photoelectron response of silicon photomultipliers," *IEEE Sensors J.*, vol. 14, no. 8, pp. 2749–2754, Aug. 2014.

[5] A. K. Jha, H. T. van Dam, M. A. Kupinski, and E. Clarkson, "Simulating silicon photomultiplier response to scintillation light," *IEEE Trans. Nucl. Sci.*, vol. 60, no. 1, pp. 336–351, Feb. 2013.

[6] D. Marano *et al.*, "Silicon photomultipliers electrical model extensive analytical analysis," *IEEE Trans. Nucl. Sci.*, vol. 61, no. 1, pp. 23–34, Feb. 2013.

[7] D. Marano *et al.*, "Improved SPICE electrical model of silicon photomultipliers," *Nucl. Instrum. Methods Phys. Res. A, Accel. Spectrom. Detect. Assoc. Equip.*, vol. 726, pp. 1–7, Oct. 2013.

[8] G. Giustolisi, G. Palumbo, P. Finocchiaro, and A. Pappalardo, "A simple extraction procedure for determining the electrical parameters in silicon photomultipliers," in *Proc. IEEE ECCTD*, Sep. 2013, pp. 1–4.

[9] G. Condorelli *et al.*, "Extensive electrical model of large area silicon photomultipliers," *Nucl. Instrum. Methods Phys. Res. A, Accel. Spectrom. Detect. Assoc. Equip.*, vol. 654, no. 1, pp. 127–134, Oct. 2011.

[10] F. Zappa, A. Tosi, A. Dalla Mora, and S. Tisa, "SPICE modeling of single photon avalanche diodes," *Sens. Actuators A, Phys.*, vol. 153, no. 2, pp. 197–204, Aug. 2009.

[11] N. Pavlov, G. Mæshlum, and D. Meier, "Gamma spectroscopy using a silicon photomultiplier and a scintillator," in *Proc. IEEE Nucl. Sci. Symp. Conf. Rec.*, Oct. 2005, pp. 173–180.

[12] S. Seifert *et al.*, "Simulation of silicon photomultiplier signals," *IEEE Trans. Nucl. Sci.*, vol. 56, no. 6, pp. 3726–3733, Dec. 2009.

[13] F. Corsi *et al.*, "Electrical characterization of silicon photo-multiplier detectors for optimal front-end design," in *Proc. IEEE Nucl. Sci. Symp. Conf. Rec.*, Oct./Nov. 2006, pp. 1276–1280.

[14] K. A. Wangerin, G.-C. Wang, C. Kim, and Y. Danon, "Passive electrical model of silicon photomultipliers," in *Proc. IEEE Nucl. Sci. Symp. Conf. Rec.*, Oct. 2008, pp. 4906–4913.

[15] F. Corsi *et al.*, "Modelling a silicon photomultiplier (SiPM) as a signal source for optimum front-end design," *Nucl. Instrum. Methods Phys. Res. A, Accel. Spectrom. Detect. Assoc. Equip.*, vol. 572, no. 1, pp. 416–418, Mar. 2007.

[16] G. Bonanno *et al.*, "Characterization measurements methodology and instrumental set-up optimization for new SiPM detectors—Part I: Electrical tests," *IEEE Sensors J.*, vol. 14, no. 10, pp. 3557–3566, Oct. 2014.

[17] G. Bonanno *et al.*, "Characterization measurements methodology and instrumental set-up optimization for new SiPM detectors—Part II: Optical tests," *IEEE Sensors J.*, vol. 14, no. 10, pp. 3567–3578, Oct. 2014.

Davide Marano was born in Catania, Italy, in 1979. He received the M.Sc. (*summa cum laude*) degree in electronics engineering from the University of Catania in 2006, and the Ph.D. degree from the Dipartimento di Ingegneria Elettrica, Elettronica e dei Sistemi, University of Catania, in 2010. Since 2012, he has been with the Osservatorio Astrofisico di Catania, Istituto Nazionale di Astrofisica, as a Junior Design Engineer. His original research projects have been focused on analog and digital integrated circuits. He has co-authored many scientific papers on mixed electronics. His main research activities include the design of low-power multistage amplifiers, high-speed buffers for liquid crystal displays, and high-performance integrated circuits and custom electronics based on field-programmable gate array.

Giovanni Bonanno was born in Catania, Italy, in 1955. He received the M.Sc. degree in physics from the University of Catania in 1980. Since 2001, he has been serving as a Full Astronomer of Astrophysical Technologies with the Osservatorio Astrofisico di Catania, Istituto Nazionale di Astrofisica. He is the co-author of several technical and scientific papers about detectors and electronic controllers, and the holder of one national patent on a photon-counting system. His main research interests and activities include silicon photomultiplier detectors, charge-coupled devices, and photon-counting systems for ground and space astrophysical applications. He has been responsible for the design and realization of electronic control systems for the instrumentation of the Italian telescope Galileo in Las Palmas, the stellar site G. Fracastoro on Mount Etna, and some space projects.

Salvatore Garozzo was born in Catania, Italy, in 1978. He received the M.Sc. degree in electronics engineering from the University of Catania in 2004, upon discussing a dissertation on AMOLED display drivers, performed at STMicroelectronics, Catania. In 2010, he was a Construction Supervisor in a company of electrical systems. Since 2006, he has been a Professor of Electronics with the Secondary High School. Since 2012, he has been with the Osservatorio Astrofisico di Catania, Istituto Nazionale di Astrofisica, as a Junior Design Engineer. His main research activities include the analysis and design of analog and mixed-signal integrated circuits. He is involved in the electronic design of high-performance integrated circuits and custom electronics based on field-programmable gate array.

Alessandro Grillo was born in Francavilla di Sicilia, Italy, in 1968. He received the M.Sc. degree in computer science from the University of Catania, in 2005. From 2006 to 2007, he was a collaborator in the project TriGrid VL (Virtual Laboratory) at the Osservatorio Astrofisico di Catania (OACT), Istituto Nazionale di Astrofisica, as a System Manager for high-performance computing (HPC)-Grid systems, developing network environments for the Theoretical Virtual Observatory implementation. From 2007 to 2011, he has collaborated with Consorzio COMETA, as a Technologist System Manager for the administration of grid computing and storage systems and the optimization of HPC environments on parallel systems based on Linux cluster. Since 2011, he has been developing software for the control interfaces of laboratory equipment in Java, C, and C++ languages. Within the activities of OACT, he has participated in the development of Web science portals and is listed as a Co-Author in several scientific publications. He often participates in conferences and meetings on specialized topics about computing and information and communications technology.

Giuseppe Romeo was born in Catania, Italy, in 1976. He received the M.Sc. degree in electronics engineering from the University of Catania in 2008, upon discussing a dissertation about output resistance adaptation in CMOS buffer amplifiers and buffers. In 2008, he received the certification of skills in electronic design of integrated circuits from the Dipartimento di Ingegneria Elettrica, Elettronica e dei Sistemi, University of Catania. In 2008, he was a Marketing Category Management Supervisor with Euronics, Italy. Since 2009, he has been a Teacher of Electronics and Mathematics in secondary schools. Since 2012, he has been a member of the Osservatorio Astrofisico di Catania, Istituto Nazionale di Astrofisica, as a Junior Design Engineer with the Laboratory Characterization of Detectors.